LETTER

Sequence analysis of mutations and translocations across breast cancer subtypes

Shantanu Banerji[1,2,3]†*, Kristian Cibulskis[1]*, Claudia Rangel-Escareno[4]*, Kristin K. Brown[5]*, Scott L. Carter[1], Abbie M. Frederick[1], Michael S. Lawrence[1], Andrey Y. Sivachenko[1], Carrie Sougnez[1], Lihua Zou[1], Maria L. Cortes[1], Juan C. Fernandez-Lopez[4], Shouyong Peng[2], Kristin G. Ardlie[1], Daniel Auclair[1], Veronica Bautista-Piña[6], Fujiko Duke[1], Joshua Francis[1], Joonil Jung[1], Antonio Maffuz-Aziz[6], Robert C. Onofrio[1], Melissa Parkin[1], Nam H. Pho[1], Valeria Quintanar-Jurado[4], Alex H. Ramos[1], Rosa Rebollar-Vega[4], Sergio Rodriguez-Cuevas[6], Sandra L. Romero-Cordoba[4], Steven E. Schumacher[1,2], Nicolas Stransky[1], Kristin M. Thompson[1], Laura Uribe-Figueroa[4], Jose Baselga[3,7], Rameen Beroukhim[1,2,3,8], Kornelia Polyak[2,3,9], Dennis C. Sgroi[3,10], Andrea L. Richardson[2,3,11], Gerardo Jimenez-Sanchez[4]†, Eric S. Lander[1,3,12], Stacey B. Gabriel[1], Levi A. Garraway[1,2,3], Todd R. Golub[1,3,13,14], Jorge Melendez-Zajgla[4], Alex Toker[3,5], Gad Getz[1], Alfredo Hidalgo-Miranda[4] & Matthew Meyerson[1,2,3,8]

Breast carcinoma is the leading cause of cancer-related mortality in women worldwide, with an estimated 1.38 million new cases and 458,000 deaths in 2008 alone[1]. This malignancy represents a heterogeneous group of tumours with characteristic molecular features, prognosis and responses to available therapy[2–4]. Recurrent somatic alterations in breast cancer have been described, including mutations and copy number alterations, notably *ERBB2* amplifications, the first successful therapy target defined by a genomic aberration[5]. Previous DNA sequencing studies of breast cancer genomes have revealed additional candidate mutations and gene rearrangements[6–10]. Here we report the whole-exome sequences of DNA from 103 human breast cancers of diverse subtypes from patients in Mexico and Vietnam compared to matched-normal DNA, together with whole-genome sequences of 22 breast cancer/normal pairs. Beyond confirming recurrent somatic mutations in *PIK3CA*[11], *TP53*[6], *AKT1*[12], *GATA3*[13] and *MAP3K1*[10], we discovered recurrent mutations in the *CBFB* transcription factor gene and deletions of its partner *RUNX1*. Furthermore, we have identified a recurrent *MAGI3–AKT3* fusion enriched in triple-negative breast cancer lacking oestrogen and progesterone receptors and *ERBB2* expression. The MAGI3–AKT3 fusion leads to constitutive activation of AKT kinase, which is abolished by treatment with an ATP-competitive AKT small-molecule inhibitor.

Breast cancers are classified according to gene-expression subtypes: luminal A, luminal B, Her2-enriched (Her2 is also known as ERBB2), and basal-like[14]. Luminal subtypes are associated with expression of oestrogen and progesterone receptors and differentiated luminal epithelial cell markers. The subtypes differ in genomic complexity, key genetic alterations and clinical prognosis[2–4,15]. To discover genomic alterations in breast cancers, we performed whole-genome and whole-exome sequencing of 108 primary, treatment-naive, breast carcinoma/normal DNA pairs from all major expression subtypes (Table 1 and Supplementary Tables 1–3), 17 cases by whole-exome and whole-genome sequencing, 5 cases by whole-genome sequencing alone, and 86 cases by whole-exome sequencing alone.

In total, whole-exome sequencing was performed on 103 tumour/normal pairs, 54 from Mexico and 49 from Vietnam, targeting 189,980 exons comprising 33 megabases (Mb) of the genome and with a median of 85.1% of targeted bases covered at least 30-fold across the sample set. This analysis revealed a total of 4,985 candidate somatic substitutions (see https://confluence.broadinstitute.org/display/CGATools/MuTect for methods and data sets) and insertions/deletions (indels, see https://confluence.broadinstitute.org/display/CGATools/Indelocator for methods) in the target protein-coding regions and the adjacent splice sites, ranging from 14 to 307 putative events in individual samples (Supplementary Table 4). These mutations represented 3,153 missense, 1,157 silent, 242 nonsense, 97 splice site, 194 deletions, 110 insertions and 32 other mutations (Supplementary Table 5). The total mutation rate was 1.66 per Mb (range 0.47–10.5) with a non-silent mutation rate of 1.27 per Mb (range 0.31–8.05), similar to previous reports in breast carcinoma[6–9]. The mutation rate in breast cancer exceeds that of haematologic malignancies and prostate cancer, but is significantly lower than in lung cancer and melanoma[10,16–19]. The most common

Table 1 | Sample collections successfully completed sequencing and analysis

Patients	Mexico N = 56	Vietnam N = 52
Median age (range)	54 (37–92)	48 (31–81)
Source of normal DNA	Blood	Adjacent tissue
Pathology subtype (percent)		
Ductal	46 (82%)	41 (79%)
Lobular	4 (7%)	0 (0%)
DCIS	0 (0%)	9 (17%)
Other	6 (11%)*	2 (4%)†
Stage		
0	0 (0%)	9 (17%)
I	8 (14%)	3 (6%)
II	36 (64%)	31 (60%)
III	12 (21%)	9 (17%)
Expression subtype (per cent)‡		
Luminal A	24 (43%)	14 (27%)
Luminal B	13 (23%)	9 (17%)
Her2	9 (16%)	12 (23%)
Basal	5 (9%)	8 (15%)
Unknown	2 (4%)	3 (6%)
Normal-like	3 (5%)	6 (11%)

* Includes tubular carcinoma, medullary carcinoma, mucinous carcinoma and mixed carcinoma (3).
† Includes mucinous carcinoma (2).
‡ Based on PAM-50 classification.
DCIS, ductal carcinoma *in situ*.

[1]The Broad Institute of MIT and Harvard, Cambridge, Massachusetts 02142, USA. [2]Department of Medical Oncology, Dana-Farber Cancer Institute, Boston, Massachusetts 02215, USA. [3]Harvard Medical School, Boston, Massachusetts 02115, USA. [4]Instituto Nacional de Medicina Genómica, Mexico City 01900, Mexico. [5]Department of Pathology, Beth Israel Deaconess Medical Center, 330 Brookline Avenue, Boston, Massachusetts 02215, USA. [6]Instituto de Enfermedades de la Mama FUCAM, Mexico City 04980, Mexico. [7]Division of Hematology and Oncology, Massachusetts General Hospital, Boston, Massachusetts 02114, USA. [8]Department of Cancer Biology, Dana-Farber Cancer Institute, Boston, Massachusetts 02215, USA. [9]Department of Medicine, Brigham and Women's Hospital, Boston, Massachusetts 02115, USA. [10]Deperment of Pathology, Massachusetts General Hospital, Boston, Massachusetts 02114, USA. [11]Department of Pathology, Brigham and Women's Hospital, Boston, Massachusetts 02115, USA. [12]Massachusetts Institute of Technology, Cambridge, Massachusetts 02139, USA. [13]Department of Pediatric Oncology, Dana-Farber Cancer Institute, Boston, Massachusetts 02215, USA. [14]Howard Hughes Medical Institute, Chevy Chase, Maryland 20815, USA. †Present addresses: Department of Medical Oncology, CancerCare Manitoba, Winnipeg, Manitoba R3E 0V9, Canada (S.B.); Global Biotech Consulting Group, Mexico City 01900, Mexico (G.J.-S.).
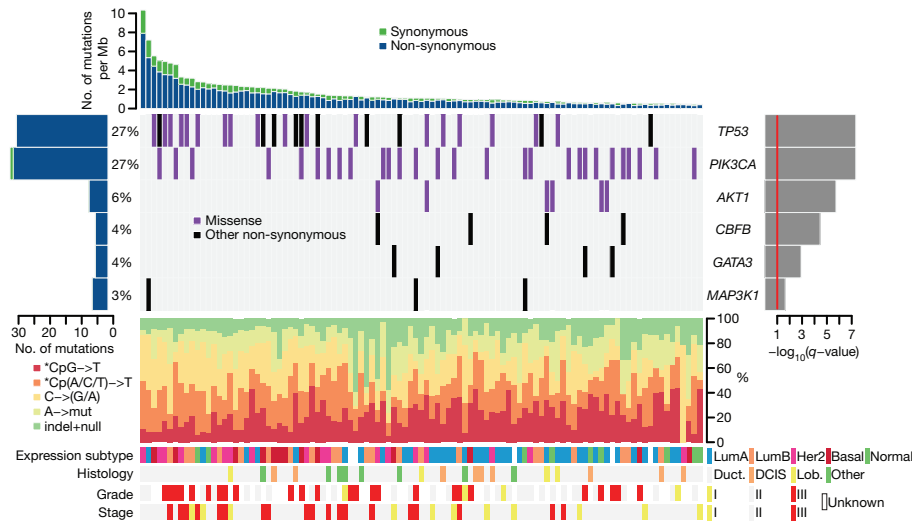*These authors contributed equally to this work.

©2012 Macmillan Publishers Limited. All rights reserved

Figure 1 | Most significantly mutated genes in breast cancer as determined by whole-exome sequencing (n = 103). Upper histogram, rates of sample-specific mutations (substitutions and indels). Green, synonymous; blue, non-synonymous. Left histogram, number of mutations per gene and percentage of samples affected (colour coding as in upper histogram). Central heat map, distribution of significant mutations across sequenced samples ('Other non-synonymous' mutations: nonsense, indel and splice-site). Right histogram, $-\log_{10}$ score of MutSig q value. Red line at $q = 0.1$. Lower chart: top, rates of non-silent mutations within categories indicated by legend; bottom, key molecular features of samples in each column. DCIS, ductal carcinoma *in situ*; Duct., infiltrating ductal carcinoma; Lob., infiltrating lobular carcinoma; Lum, luminal.

mutation events observed are C to T transition events in CpG dinu-cleotides (Fig. 1 and Supplementary Fig. 4).

We performed validation experiments on 494 candidate mutations (representing all significantly mutated genes and genes in significantly mutated gene sets) using a combination of mass-spectrometric geno-typing, 454 pyrosequencing, Pacific Biosciences sequencing and Illumina sequencing of matched formalin-fixed paraffin-embedded tissue, and confirmed the presence of 94% of protein-altering point mutations (Supplementary Table 4 and Supplementary Fig. 5); this validation rate is consistent with previous results that 95% of point mutations can be validated with orthogonal methods[16,17]. Only 18 out of 39 (46%) indels among significantly mutated genes were confirmed.

Six genes were found to be mutated with significant recurrence in the 103 whole-exome sequenced samples, by analysis with the MutSig algorithm[16,17] (https://confluence.broadinstitute.org/display/CGATools/MutSig) at a false discovery rate (FDR) < 0.1 after correction for mul-tiple hypothesis testing (Supplementary Table 6a), manual review of reads, and subsequent orthogonal confirmation of somatic events (Fig. 1 and Supplementary Fig. 6). One gene, *CBFB*, is identified for the first time as a significantly mutated gene in breast cancer or any other epithelial cancer, to our knowledge, whereas the other five genes (*TP53*, *PIK3CA*, *AKT1*, *GATA3* and *MAP3K1*) have previously been reported as mutated in breast cancer[7,10,13]. This significantly mutated genes list, as any list produced by a statistical method, is probably incomplete and reflects the statistical power of our cohort size—larger sample sets will provide further statistical power.

Somatic mutations in *TP53* and *PIK3CA* were each present in 27% of samples, consistent with published frequencies[10,20] (Fig. 1). *TP53* mutations occur in samples with a higher mutation rate (*t*-test $P = 0.0079$ comparing samples with mutation rates greater than or less than the median 1.66 mutations per Mb) and were distributed across the gene in sites reported in COSMIC (http://www.sanger.ac.uk/genetics/CGP/cosmic/). Also, using the ABSOLUTE algorithm for determining allele-specific copy number[21], we observed that 21 out of 31 *TP53* mutations were homozygous (Supplementary Table 4). *PIK3CA* mutations were clustered in the helical (amino acids 542/545; 40%) and kinase domains (amino acid 1047; 47%)[20]. Six samples harboured the *AKT1* E17K mutation that alters the pleckstrin-homology (PH) domain and leads to activation of the kinase[12].

AKT1 and *PIK3CA* mutations, which activate the phosphatidylinositol-3-kinase (PI3K) pathway, were mutually exclusive in our data set. *MAP3K1*, recently reported as mutated in oestrogen-receptor-positive breast cancers[10], harboured five mutations in three patients with oestrogen-receptor-positive disease, and followed a pattern consistent with positive selection for recessive inactivation of the gene. In total, two frameshift, two nonsense and one missense mutation, combined with a homozygous deletion spanning the coding region were observed. Although the point mutations seemed to be heterozygous by copy-number analysis, two patients harboured dual mutations, consistent with compound heterozygous inactivation, although con-firmatory phasing data were not available. The *GATA3* transcription factor gene harboured mutations in four patients with luminal tumours, including three previously unknown frameshift mutations near the 3′-end of the coding sequence. We also identified one previ-ously described splice-site mutation that disrupts zinc-finger domains in GATA3 required for DNA binding[13].

CBFB, encoding the core-binding-factor beta subunit, was mutated in four oestrogen-receptor-positive samples, with one nonsense muta-tion and three truncating frameshift mutations (Fig. 2a). *CBFB* somatic mutations have been noted in isolated cases of breast cancer[6,10]. This is the first report of these mutations recurring at a significant rate above background; the sample size is not sufficient to determine whether these mutations are specific for oestrogen-receptor-positive subtypes. *CBFB* encodes the non-DNA-binding component of a heterodimeric protein complex, together with the DNA-binding RUNX proteins encoded by *RUNX1*, *RUNX2* and *RUNX3*. Copy-number analysis, using the ABSOLUTE algorithm[21], provides further evidence for loss of function of the RUNX1/CBFB complex in breast cancer: the cases with *CBFB* mutations seem to have hemizygous deletions of one par-ental allele, whereas two additional cases harbour homozygous dele-tions of *RUNX1* (Fig. 2b, c and Supplementary Figs 7 and 8). Oncogenic rearrangements of *RUNX1* or *CBFB* are common in acute myeloid leukaemia[22,23] (including the *CBFB–MYH11* translocation believed to have dominant negative function[22]). This is to our know-ledge the first report of inactivation of this transcription factor com-plex in epithelial cancers.

Significance analysis restricted to somatic mutations in genes reported in COSMIC revealed three significantly mutated genes,
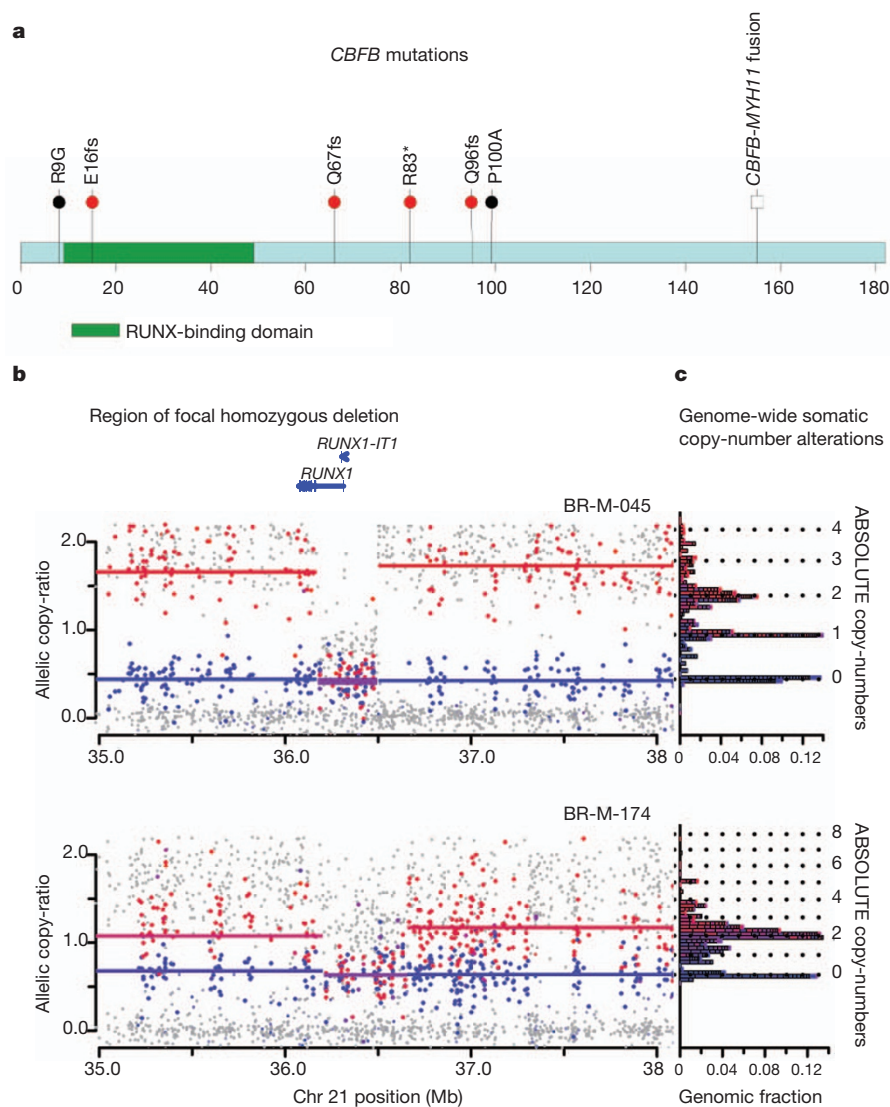
Figure 2 | *CBFB* mutations and *RUNX1* deletions. **a**, *CBFB* coding region diagram, RUNX-binding domain in green. Mutations identified in this study (red bullets), previously identified mutations[6,10] (black bullets), and known *CBFB–MYH11* fusion indicated. **b**, Allelic copy ratios for the 3-Mb region surrounding *RUNX1* in samples BR-M-045 and BR-M-174. Dots indicate copy-ratios for individual SNP alleles. Red, higher copy-ratio allele for informative SNPs that are heterozygous in matched normal DNA; blue, lower-copy ratio SNPs; grey, uninformative SNPs (homozygous in matched normal). Lines indicate inferred segmental copy-ratios. Red, higher-copy segment; blue, lower-copy segment; purple, equal-copy segment. **c**, Histogram depicting bins of segmented copy number (*y* axis), with inferred integral copies shown by dotted lines; the length of each horizontal block corresponds to the fraction of the haploid genome at the copy number level, or 'genomic fraction' (*x* axis).

PIK3CA, *TP53* and *ERBB2*, the latter below the significance threshold in the complete analysis (Supplementary Table 7). *ERBB2* contained somatic mutations in three samples, with two being identical S310F mutations (these two samples are distinct on the basis of their germline and somatic genotypes). The S310F mutation can activate ERBB2 and is transforming *in vitro* (personal communication from H. Greulich). Neither sample with the S310F activating mutation has *ERBB2* amplification (Supplementary Fig. 9). The two samples belong to the Her2-enriched and luminal B subtypes, which typically have *ERBB2* amplification; this supports the notion that the observed mutations have a driving role in these tumours[10,24].

To identify candidate genomic rearrangements, we applied the dRanger algorithm[16,17] to the 22 cases with paired tumour/normal whole-genome sequencing data (Supplementary Table 8). The rate of rearrangements ranged from a median of 30 rearrangements per sample in the luminal A subtype (range 0–218) to the basal-like and Her2-enriched subtypes with a median of 237 and 246 rearrangements, respectively (Supplementary Fig. 10); the rates are similar to a recent report[15]. We performed polymerase chain reaction (PCR)

amplification on a subset of the candidate rearrangements (Supplementary Methods) and confirmed 89 out of 165 events (54%). No rearrangement was seen in more than one sample (Supplementary Table 8). In addition, we did not identify rearrangements previously observed by DNA sequencing[15] nor by complementary DNA (cDNA)-sequencing, including MAST and NOTCH family-gene fusions[25].

The discovery of recurrent driver rearrangements in other epithelial cancers[26,27] led to a closer examination of the list of confirmed rearrangements. In a triple-negative, basal-like subtype tumour, we observed a rearrangement between the genes *MAGI3* (membrane-associated guanylate kinase, WW and PDZ domain containing 3) on chromosome 1p and *AKT3* (v-akt murine thymoma viral oncogene homologue 3) on chromosome 1q, resulting in a balanced transloca-tion from intron 9 in *MAGI3* to intron 1 of *AKT3* (Fig. 3a). The previously unknown fusion genes were confirmed in tumour DNA by sequencing the product of PCR amplification (Fig. 3b). The *MAGI3* disruption is complemented by a hemizygous deletion of the other allele (Supplementary Fig. 11a). The expression levels of indi-vidual exons of *MAGI3* and *AKT3* correspond to the predicted
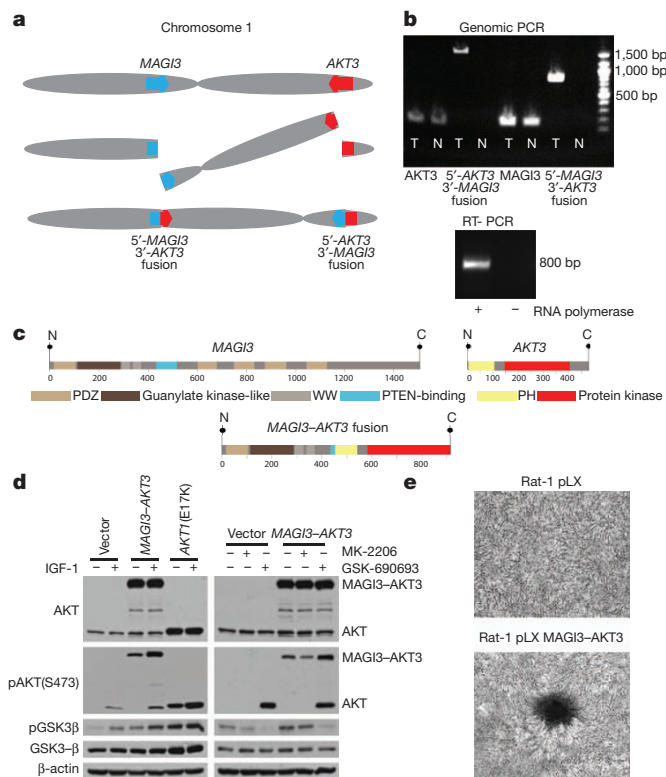
Figure 3 | MAGI3–AKT3 fusion gene. a, Diagram of balanced translocation between *MAGI3* and *AKT3*. **b**, Top, genomic DNA PCR for *AKT3*, *MAGI3* and both fusion products in tumour (T) and normal (N). Bottom, cDNA PCR of fusion gene in tumour. **c**, Above, MAGI3 and AKT3 protein domains; below, putative fusion protein. **d**, Immunoblots of lysates from ZR-75 cells transfected with vector, *MAGI3–AKT3* fusion, or *AKT1* E17K mutant, grown in low-serum media, for the indicated antibodies. Left, infected cells with and without insulin growth factor 1 (IGF-1) stimulation; right, treatment of vector or *MAGI3–AKT3* overexpressing cells with AKT inhibitors MK-2206 and GSK-690693. **e**, Focus formation assays with Rat-1 cells expressing pLX control or *MAGI3–AKT3*, and stained with crystal violet.

5′-*MAGI3–AKT3*-3′ fusion (Supplementary Fig. 11b), with this sample having the highest *AKT3* expression in the data set. Expression of the fusion gene was confirmed in the tumour sample by PCR amplification of the cDNA (Fig. 3b).

The rearrangement produces an in-frame fusion gene with a predicted MAGI3–AKT3 fusion protein that combines MAGI3 lacking the second PDZ domain, reported to bind to PTEN and be required for the inhibitory effect of PTEN on the PI3K pathway[28], together with an AKT3 region that retains an intact kinase domain but has a disruption of the pleckstrin homology domain before the glutamate at position 17 (Fig. 3c). *AKT3* shares significant homology to *AKT1* and is reported to be the dominant AKT family member expressed in hormone-receptor-negative breast cancers[29]. Together, the *MAGI3–AKT3* translocation and deletion of *MAGI3* could result in the combined loss of function of a tumour suppressor gene (*PTEN*) and activation of an oncogene (*AKT3*).

To evaluate oncogenic activity of the *MAGI3–AKT3* fusion, we expressed the fusion gene ectopically in ZR-75 cells. The MAGI3–AKT3 fusion protein is constitutively phosphorylated at serine 473 in the AKT3 kinase domain (numbered according to the wild-type protein) in the absence of growth factors (Fig. 3d); ectopically expressed AKT1 with an engineered E17K mutation is likewise constitutively phosphorylated (Fig. 3d), as previously reported[12]. Constitutive activation of the MAGI3–AKT3 kinase in turn activates downstream pathways as demonstrated by phosphorylation of GSK3β, an AKT substrate (Fig. 3d). Phosphorylation of GSK3β by the MAGI3–AKT3 fusion can be inhibited with an ATP-competitive

small molecule AKT inhibitor, GSK-690693, but not with an allosteric AKT inhibitor, MK-2206, that interacts with the PH domain of AKT (Fig. 3d). Overexpression of the *MAGI3–AKT3* fusion gene in Rat-1 fibroblast cell lines led to loss of contact inhibition and focus formation (Fig. 3e).

We screened 235 additional breast cancer samples for the presence of the 5′-*MAGI3–AKT3*-3′ fusion event by PCR with reverse transcription (RT–PCR) of cDNA followed by Sanger sequencing of breakpoints. The fusion was present in 8 of the 235 samples, including 5 out of 72 triple-negative (oestrogen-receptor-, progesterone-receptor- and Her2-negative) samples (Supplementary Fig. 12).

The power provided by whole-genome and whole-exome sequencing of a relatively large and diverse breast cancer sample set has enabled several significant discoveries, including the identification of recurrent inactivating mutations in *CBFB* and of a recurrent translocation of *MAGI3–AKT3*. The mutations in *CBFB*, *RUNX1* and *GATA3* suggest the importance of understanding epithelial cell differentiation and its regulatory transcription factors in breast cancer pathogenesis. The recurrent genomic fusion involving *AKT3* suggests that the use of ATP-competitive AKT inhibitors should be evaluated in clinical trials for the treatment of fusion-positive triple-negative breast cancers, a subtype where limited therapeutic options exist beyond systemic cytotoxic chemotherapy.

METHODS SUMMARY

All samples were obtained under institutional IRB approval and with documented informed consent. Breast cancer specimens from Mexico were paired with peripheral blood normal DNA whereas the Vietnamese samples were paired with DNA from normal adjacent breast tissue. Tumour RNA for each case was analysed on exon arrays to determine breast cancer expression subtype using the PAM50 classification method, whereas tumour/normal DNA pairs were analysed for copy number, allelic imbalance, and ancestry using single nucleotide polymorphism (SNP) arrays. A total of 108 samples, 17 both whole-genome sequencing and whole-exome sequencing, 86 whole-exome sequencing only, and 5 whole-genome sequencing only, passed initial qualification metrics, library construction, and successfully achieved desired sequencing depth (100× whole-exome sequencing; 30× whole-genome sequencing) on the Illumina sequencing platform (Supplementary Figs 1–3, Supplementary Tables 2 and 3). Tumour-specific point mutations, small insertions/deletions (indels), and rearrangements were detected by comparing tumour DNA to its paired normal DNA and using a series of algorithms to identify somatic events (Supplementary Fig. 2)[16,17]. Additional mutation calling was performed separately on tumour and normal DNA to identify germline mutation events that may confer susceptibility to breast carcinoma. Allele-specific copy number of each gene/mutation was determined using the HAPSEG and ABSOLUTE analysis methods. Confirmation of point mutations and indels was performed using mass-spectrometry-based genotyping and orthogonal next-generation sequencing methods, whereas putative in-frame genomic rearrangements were PCR-amplified from DNA to confirm the presence of the event.

A complete description of the materials and methods is provided in the Supplementary Information. Access to the data and computational algorithms used in this study can be found at https://confluence.broadinstitute.org/display/CGATools/Home.

1. Jemal, A. *et al.* Global cancer statistics. *CA Cancer J. Clin.* **61**, 69–90 (2011).
2. Sørlie, T. *et al.* Gene expression patterns of breast carcinomas distinguish tumor subclasses with clinical implications. *Proc. Natl Acad. Sci. USA* **98**, 10869–10874 (2001).
3. Chin, K. *et al.* Genomic and transcriptional aberrations linked to breast cancer pathophysiologies. *Cancer Cell* **10**, 529–541 (2006).
4. Gatza, M. L. *et al.* A pathway-based classification of human breast cancer. *Proc. Natl Acad. Sci. USA* **107**, 6994–6999 (2010).
5. King, C. R., Kraus, M. H. & Aaronson, S. A. Amplification of a novel v-*erb*B-related gene in a human mammary carcinoma. *Science* **229**, 974–976 (1985).
6. Sjöblom, T. *et al.* The consensus coding sequences of human breast and colorectal cancers. *Science* **314**, 268–274 (2006).
7. Wood, L. D. *et al.* The genomic landscapes of human breast and colorectal cancers. *Science* **318**, 1108–1113 (2007).
8. Shah, S. P. *et al.* Mutational evolution in a lobular breast tumour profiled at single nucleotide resolution. *Nature* **461**, 809–813 (2009).
9. Ding, L. *et al.* Genome remodelling in a basal-like breast cancer metastasis and xenograft. *Nature* **464**, 999–1005 (2010).

10. Kan, Z. *et al.* Diverse somatic mutation patterns and pathway alterations in human cancers. *Nature* **466,** 869–873 (2010).
11. Samuels, Y. *et al.* High frequency of mutations of the *PIK3CA* gene in human cancers. *Science* **304,** 554 (2004).
12. Carpten, J. D. *et al.* A transforming mutation in the pleckstrin homology domain of AKT1 in cancer. *Nature* **448,** 439–444 (2007).
13. Usary, J. *et al.* Mutation of *GATA3* in human breast tumors. *Oncogene* **23,** 7669–7678 (2004).
14. Sorlie, T. *et al.* Repeated observation of breast tumor subtypes in independent gene expression data sets. *Proc. Natl Acad. Sci. USA* **100,** 8418–8423 (2003).
15. Stephens, P. J. *et al.* Complex landscapes of somatic rearrangement in human breast cancer genomes. *Nature* **462,** 1005–1010 (2009).
16. Berger, M. F. *et al.* The genomic complexity of primary human prostate cancer. *Nature* **470,** 214–220 (2011).
17. Chapman, M. A. *et al.* Initial genome sequencing and analysis of multiple myeloma. *Nature* **471,** 467–472 (2011).
18. Pleasance, E. D. *et al.* A comprehensive catalogue of somatic mutations from a human cancer genome. *Nature* **463,** 191–196 (2010).
19. Pleasance, E. D. *et al.* A small-cell lung cancer genome with complex signatures of tobacco exposure. *Nature* **463,** 184–190 (2010).
20. Bachman, K. E. *et al.* The *PIK3CA* gene is mutated with high frequency in human breast cancers. *Cancer Biol. Ther.* **3,** 772–775 (2004).
21. Carter, S. L. *et al.* Absolute quantification of somatic DNA alterations in human cancer. *Nature Biotechnol.* doi:10.1038/nbt.2203 (29 April 2012).
22. Cameron, E. R. & Neil, J. C. The *Runx* genes: lineage-specific oncogenes and tumor suppressors. *Oncogene* **23,** 4308–4314 (2004).
23. Shigesada, K., van de Sluis, B. & Liu, P. P. Mechanism of leukemogenesis by the inv(16) chimeric gene *CBFB/PEBP2B-MHY11*. *Oncogene* **23,** 4297–4307 (2004).
24. Stephens, P. *et al.* Lung cancer: intragenic ERBB2 kinase mutations in tumours. *Nature* **431,** 525–526 (2004).
25. Robinson, D. R. *et al.* Functionally recurrent rearrangements of the MAST kinase and Notch gene families in breast cancer. *Nature Med.* **17,** 1646–1651 (2011).
26. Soda, M. *et al.* Identification of the transforming *EML4–ALK* fusion gene in non-small-cell lung cancer. *Nature* **448,** 561–566 (2007).
27. Tomlins, S. A. *et al.* Recurrent fusion of *TMPRSS2* and ETS transcription factor genes in prostate cancer. *Science* **310,** 644–648 (2005).
28. Wu, Y. Interaction of the tumor Suppressor PTEN/MMAC with a PDZ domain of MAGI3, a novel membrane-associated guanylate kinase. *J. Biol. Chem.* **275,** 21477–21485 (2000).
29. Nakatani, K. *et al.* Up-regulation of Akt3 in estrogen receptor-deficient breast cancers and androgen-independent prostate cancer lines. *J. Biol. Chem.* **274,** 21528–21532 (1999).

Supplementary Information is linked to the online version of the paper at www.nature.com/nature.